Sensing and Bio-Sensing Research 41 (2023) 100566

Contents lists available at ScienceDirect

Sensing and Bio-Sensing Research

journal homepage: www.elsevier.com/locate/sbsr

Rapid detection of tetracycline residues at clinically relevant levels via a novel, inexpensive and analytically-sensitive magneto-immunoassay – A feasibility study

Owen J. Harrison [a], Bertrand Monnier [b], Ed Regan [c], Dave West [c], Hugh Ballantine Dykes [c], Jeffrey S. Davey [a], Janice Kiely [a], Richard Luxton [a,*]

[a] Institute of Bio-Sensing Technology, University of the West of England, Bristol BS16 1QY, UK
[b] Centre for Research in Biomedicine, University of the West of England, Bristol BS16 1QY, UK
[c] MIATech BioSolutions, Porton Science Park, Porton Down, Salisbury SP40BF, UK

ARTICLE INFO

Keywords:
Magneto-immunoassay
Magnetometer
Biosensor
Paramagnetic particles
Tetracycline
Antibiotic detection

ABSTRACT

Expensive, time-consuming and labour-intensive solvent-extraction and liquid-chromatography methods are the industry's current gold standard for antibiotic residue quantification. A novel immunoassay methodology and system for the rapid detection of clinically relevant levels of tetracycline residues found in food-producing animal tissues is described. Anti-tetracycline antibody-coated paramagnetic particles were used for the specific capture of tetracycline in spiked buffer (with and without a 1% pork muscle tissue suspension) and quantified via an analytically-sensitive in-house magnetometer instrument. Detection of tetracycline between 0.1 μg/mL - 1 μg/mL was achieved, with a readout time (including sample treatment) presented in 20 min. The magneto-immunoassay described provides a rapid, low-cost, de-skilled and analytically-sensitive solution for tetracycline screening at the point-of-sampling, with potential applications for other prevalent antibiotic families used in the international farming and food industry.

1. Introduction

Antibiotics have been used for therapy, prophylaxis and growth promotion in livestock since the 1940s [1]. The tetracycline (TC) family was one of the first antibiotic groups to be widely utilised for these purposes [1]. By preventing attachment of aminoacyl-tRNA to bacterial ribosomes, tetracyclines are able to inhibit protein synthesis of a wide range of gram-positive and gram-negative bacteria, in addition to a host of atypical organisms [1–3]. Administered at sub-therapeutic levels, tetracyclines and other antibiotics work to minimise the intestinal load of bacteria and reduce competition for nutrient uptake in the gastrointestinal tract [1–3]. Biosynthesis of vitamins is increased, immune function is heightened and metabolism is boosted [1–3]. This broad-spectrum mode of action cemented antibiotic use despite links to rising antibiotic resistance and government legislation [1–3]. To restrict overuse and ensure the lowest possible consumer exposure, maximum antibiotic residue limits (MRLs) in animal tissues were introduced [4–6]. The acceptable limit of TC in livestock is between 100 μg/kg – 600 μg/kg (EU) depending on tissue origin [7–9]; residues above this threshold can be harmful to human health and fuel antibiotic resistance [7–9]. The Rapid Alert System for Food and Feed works to evaluate and control these risks as well as maintain food safety levels for the general public [7–9]. In accordance, tissue sample analysis and screening is integral and thus the need for reliable, accurate and sensitive antibiotic detection systems [10–12].

Two types of analytical method exist for the detection and determination of antibiotic residues in animal samples; confirmatory and screening [10–12]. High-performance liquid chromatography (HPLC) is the industry's current gold standard for all antibiotic detection and is utilised in 60% of cases due to its superior selectivity and sensitivity [10–12]. Despite the benefits of HPLC and other confirmatory techniques such as LC-mass spectrometry and thin-layer chromatography [10–12], these methods require complex sample clean-up and extraction phases in addition to costly equipment and reagents [10–12]. Biosensor-based tests (employed in only 3–8% of cases) are consequently on the rise, with increasing demand and a total yearly investment of $300 m (€236 m) into research and development [10–12]. Unlike chromatography-based quantification, biosensors do not require time-

* Corresponding author.
E-mail address: Richard.Luxton@uwe.ac.uk (R. Luxton).

https://doi.org/10.1016/j.sbsr.2023.100566
Received 11 August 2020; Received in revised form 20 July 2021; Accepted 22 May 2023
Available online 25 May 2023

consuming pre-measurement processing or skilled operators, making them ideal for high-throughput and routine use [10–12].

Increased demand for quicker sample analysis, screening capabilities and cheaper alternatives has highlighted the need for simplified and inexpensive antibiotic detection at the samples' source e.g. slaughterhouses, farms and processing plants [10–12]. Development of new immunoassay formats (frequently used in biosensor-based systems) are addressing this demand, resulting in shorter assay times and greater sensitivity. Despite these advances, matrix fouling effects, signal quenching and sample contamination persist within conventional immunoassays [13–15]. The use of paramagnetic particles (PMPs), 0.1–5 μm spheres containing colloidal iron-oxide with magnetic field dependent magnetisation has alleviated many of these issues [13–15]. Due to their inherent stability, paramagnetic properties, ease of manipulation and functionalisation, PMPs are ideal for rapid immunoassay-based detection systems within complex matrices [13–15]. In response, several PMP detection technologies, such as magnetic frequency mixing coils [16], cantilever devices [17] as well as magnetoresistance [18] and Hall sensors [19], have since been developed.

The magnetometer device described here and in previous work by the authors [13–15,20] utilises a highly-sensitive resonant coil sensor to accurately detect PMPs. Positioned adjacently to the sensor surface that lies beneath the base of a reaction vessel, the resonant coil is able to directly detect PMP presence through magnetic field disturbances [13,20]. In response, a registered change in the inductance of the sensor occurs, causing a measurable resonant frequency variation due to the phase-locked loop circuitry of the magnetometer [13,20]. By fixing an adapted neodymium magnet onto a motorised platform perpendicular to the coil and underneath the sensor surface, PMPs can be rapidly pulled down onto reaction vessel surfaces [13,20]. Competition of the analyte of interest found within the sample against analyte immobilised on reaction vessel surfaces for binding sites on antibody (Ab)-coated PMPs (Ab-PMPs) forms the basis of the magneto-immunoassay (MIA) [20]. PMPs conjugated with corresponding Ab (with a known and limited number of active sites) are inhibited from binding to analyte-coated surfaces if analyte is present within the sample [13,20]. Variations in the output voltage, corresponding to resonant frequency changes, occur in response to PMP-sensor surface binding events enable specific quantification of sample analyte concentrations (Fig. 1) [13,20]. The magnetometer and reaction vessel (Fig. 2) are compact, built from inexpensive components and can be readily deployed in the field providing a novel alternative solution to point-of-sampling diagnostics [13,20].

The research described is an 18-month feasibility study focused on developing and optimising the existing MIA biosensor-based technology for the purpose of antibiotic detection. The proposed technique aimed to

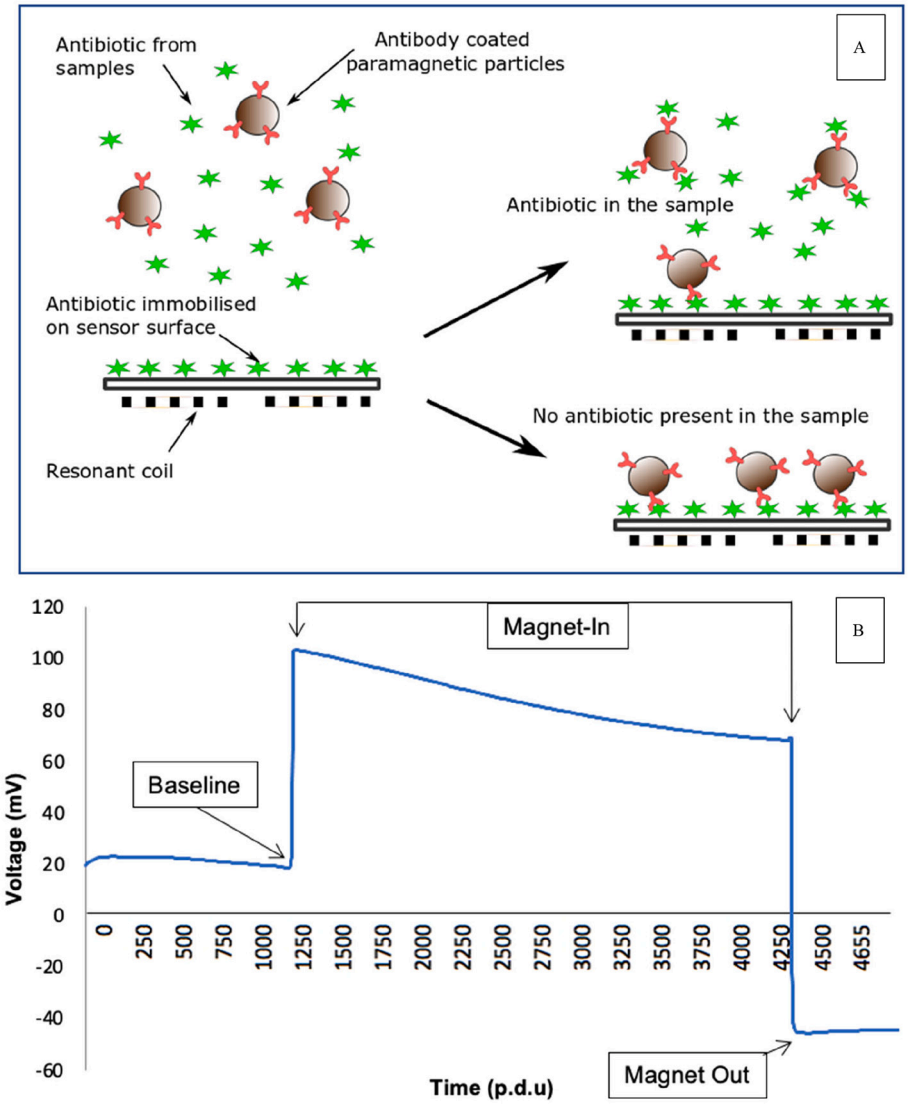

Fig. 1. (A) a schematic representation of the magneto-immunoassay. (B) A typical magnetometer trace in response to antibody-coated paramagnetic particles (Ab-PMPs) after a 5-min Magnet-In period on antigen-coated reaction vessel surfaces. In the presence of antibiotic within sample solutions, Ab-PMPs are inhibited from binding to the antibiotic-coated reaction vessel surface. In the absence of antibiotic in sample solutions, Ab-PMPs are free to bind to the sensor surface, resulting in a measurable shift in voltage recorded by the magnetometer. The relative change in voltage can be used to quantify the concentration of antibiotic in sample solutions. Under control conditions, upon retraction of the magnet (Magnet-Out), trace readings return to Baseline levels. Under experimental conditions (as shown in (B)), a measurable shift from Baseline occurs which can be used to quantify surface-bound PMPs.

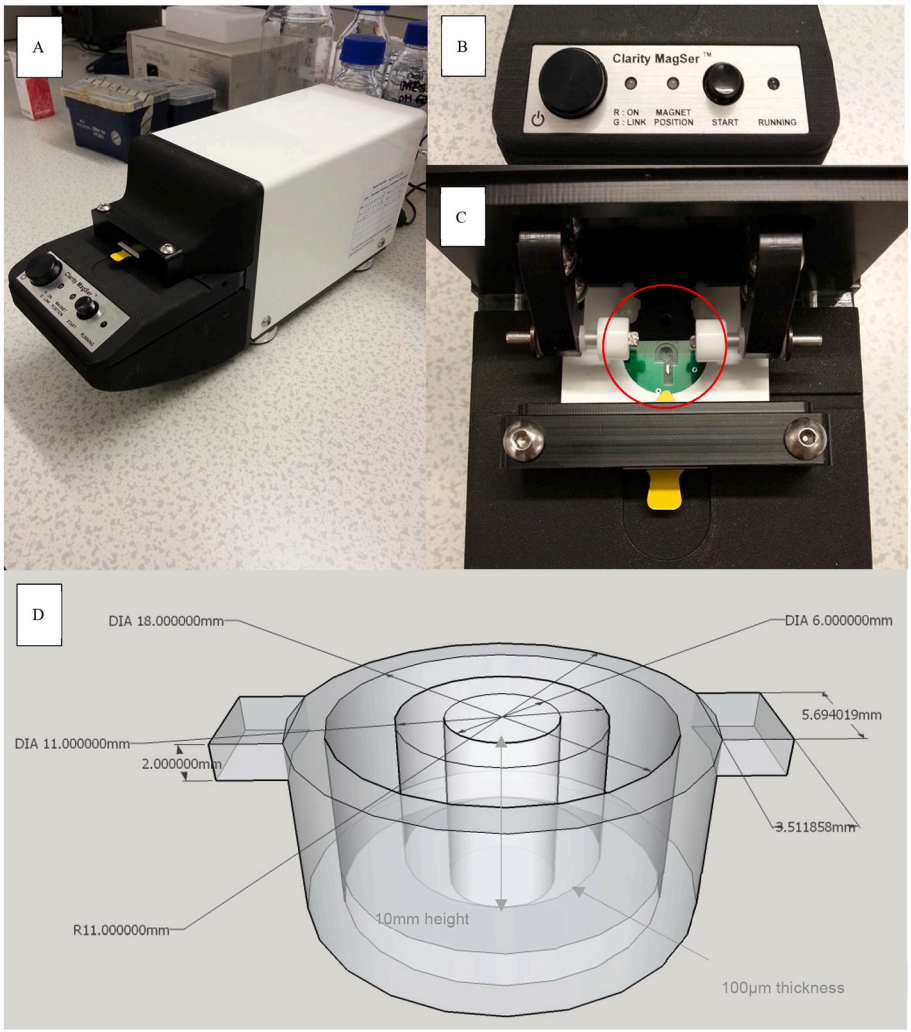

Fig. 2. The magnetometer device and reaction vessel: (A) Magnetometer overview and overall size. The removable white enclosure houses the resonant coil and power circuitry as well as an AC/DC converter; (B) Magnetometer heads-up display. Two buttons, on/off and start, in addition to LEDs which emit red (device on), green (device-computer connectivity), white (magnet in) and/or blue (programme running) light, functioning as on-board status indicators; (C) Magnetometer sensor interface. To load the reaction vessel, the yellow toggle is pulled to give access to the enclosure. The reaction vessel is loaded into position (red circle) and rests directly above the resonant coil. Clamps on either side drop in and secure the reaction vessel once inserted; (D) Orthographic projection of the reaction vessel design. DIA = diameter; R = radius. (For interpretation of the references to colour in this figure legend, the reader is referred to the web version of this article.)

provide an on-site, de-skilled, rapid, low-cost screening test solution for detection of TC at clinically relevant levels found in livestock. This paper describes the use of the novel magnetic detector to effectively quantify TC within the defined MRL in spiked buffer and a 1% meat suspension. Key findings and developments are detailed and the feasibility of the proposed system for clinical application at the point-of-sampling is discussed.

2. Materials and methods

2.1. Solution and sample preparation

All chemicals were purchased from Sigma Aldrich (UK) unless otherwise stated. Assay buffer was formed of 1% Bovine Serum Albumin (BSA) and 0.05% Tween-20 in a phosphate buffed saline (PBS) solution. TC was solubilised in 70% ethanol, stored at −20 °C and diluted in assay buffer when specific assay concentrations were required. Estapor PMPs (164 nm, 294 nm and 460 nm) were purchased from Merck, UK. Dynabeads® MyOne™ tosyl-activated PMP (ThermoFisher Scientific, UK; selected for assay development and optimisation) stock (100 mg/mL)) was diluted 1:4 in MES + 0.5% Tween-20 and 0.2% sodium azide buffer solution (pH 5.5) and stored in glass vials at 4 °C. Once functionalised (see: Preparation of antibody-coated PMPs), anti-TC Ab-PMP stock was pulse sonicated (Microson XL 2000 Ultrasonic Liquid Processor) on ice at 10 amplitude microns (Aμ) for 4x30s with 60s cooling intervals. For the matrix-effect experiments, UK-reared pork produced to RSPCA welfare standards of pork was used. 1.0 g of pork muscle tissue was added to 50 mL of 1× PBS and pulse sonicated on ice at 10 Aμ for 5 × 30 s with 2-min gaps between pulses. Prior to each assay, anti-TC Ab-PMP stock was vortexed for 30s and diluted in assay buffer to achieve the concentrations required for each assay.

2.2. Preparation of antibody-coated PMPs

All PMP solutions were vortexed for >30s or tilted/rotated for 5 min prior to each stage described below to ensure homogeneity. 600 μL of PMP stock (25 mg/mL) was transferred into a 1.5 mL tube and placed on the magnetic rack (DynaMag-2 Magnet) for 1–2 min. The supernatant was removed, 0.5 mL of 0.1 M sodium borate coating buffer (pH 9.5) was added. The tube was placed on the magnet rack for a further 1–2 min; the supernatant was discarded and 150 μL 0.1 M sodium borate coating buffer (pH 9.5) was added. 50 μL of the now washed PMPs (5 mg) were added into a new 1.5 mL tube and a volume of 0.1 M sodium borate coating buffer (pH 9.5) was added depending on antibody coat percentages. Primary monoclonal mouse anti-tetracycline antibody (mAb anti-TC; 2BScientific, UK) was added at various *w/v* ratios to achieve 0.5–2% antibody surface coating on PMPs, with the remaining 98–99.5% made up from a volume of 0.1% BSA in 0.1 M sodium borate coating buffer (pH 9.5); a total recommended protein concentration of 200 μg protein (40 μg protein/mg beads). 20 μL of mAb anti-TC (concentration dependent on Ab-% coating) was added. 415 μL of 3 M ammonium sulphate stock solution (pH 9.5) was added and the tube was

pulse sonicated on ice at 10Aμ for 4x30s with 60s cooling intervals. The tube was then incubated for 3.5 h at 37 °C with slow tilt rotation (Dynabeads® MX1 Mixer). After incubation, the tube was re-sonicated; incubation was continued for a further 20 h. The following day, the tube was placed on the magnet rack for 1–2 min; the supernatant was removed. The same total volume (1250 μL) of PBS + 0.5% BSA + 0.05% Tween-20 was added and the tube was incubated at 37 °C overnight.

The following day the tube was placed on the magnetic rack for 1–2 min; the supernatant was removed. A volume of 0.5 mL of PBS + 0.1% BSA + 0.05% Tween-20 [wash/storage buffer] was added and the now functionalised PMPs (anti-TC Ab-PMPs) were re-suspended; this was repeated to give a total of 3 washes. Anti-TC Ab-PMPs were then re-suspended and made up to 1000 μL in wash/storage buffer and re-sonicated. A 1:500 dilution of anti-TC Ab-PMPs in wash/storage buffer was prepared. 20 μL of the 1:500 dilution was pipetted into a haemocytometer; up to 8 squares were imaged. Anti-TC Ab-PMPs were then counted using the multi-point function on ImageJ [21]. Confirmation of antibody conjugation onto anti-TC Ab-PMPs was achieved through incubation of anti-TC Ab-PMPs with secondary rabbit anti-mouse IgG-HRP conjugate (sAb anti-mouse; Dako, UK) and tetramethylbenzidine (TMB). In the presence of HRP, TMB (a chromogenic compound) is oxidised and produces a colorimetric derivative, the intensity of which was used to compare against a colorimetric standard curve to infer the level of conjugated antibody on Ab-PMPs.

2.3. Reaction vessel design

The specific dimensions and materials used for the reaction vessel were critical to assay functionality. The total volume (200 μL) and height of the central column (10 mm) promoted optimal PMP kinetics, whilst the thickness at the base of the reaction vessel (100 μm) ensured surface-bound PMPs were accurately detected by the resonant coil (Fig. 2). Given its high tensile strength, in future work, sample preparation via sonication of tissue and anti-TC Ab-PMPs (leading to lysis, TC release and subsequent capture by PMPs) could be conducted within the reaction vessel.

2.4. Reaction vessel surface treatment

A 40 μL volume of a 1:2 dilution of Mix&Go in PBS (commercial surface activation agent; One World Labs, USA) was loaded onto reaction vessel surfaces, tapped to ensure total surface coverage and incubated for 1 h at room temperature. Reaction vessels were then washed (x2) with 200 μL PBS and once with 200 μL dH_2O. BSA-TC stock [20 mg/mL] (Bioquote, UK) was added to PBS to make the specified assay concentration. 50 μL of BSA-TC was pipetted into reaction vessels and PBS into negative controls. Reaction vessels were incubated at 4 °C in humidified conditions overnight. The following day, liquid inside reaction vessels was removed and washed (200 μL x3) in PBS + 0.05% Tween-20 [wash buffer]. Reaction vessels were then blocked and incubated for 2 h in PBS + 1% BSA [blocking buffer] at 4 °C. After incubation, liquid inside reaction vessels was removed and ready for use in assays.

2.5. Magneto-immunoassay

A schematic diagram for detection of TC via the MIA is shown in Fig. 3. PMPs were coated with anti-TC antibody whilst reaction vessel surfaces were coated with BSA-TC. The extent of competitive inhibition in the MIA was determined by the level of TC present within a given sample.

A volume of 200 μL of sonicated anti-TC Ab-PMPs was pipetted into a 1.5 mL tube and placed on the magnetic rack for 1–2 min. The supernatant was removed and 200 μL of TC at the specified concentration was added into the tube. The tube was vortexed for precisely three minutes; a preliminary method in which to mimic the conditions and dynamics of the final assay when applied to livestock tissue, whereby tissue lysis occurs (following sonication in the presence of anti-TC Ab-PMPs) leading to TC release and subsequent capture by anti-TC Ab-PMPs before the start of magnetometer cycling. After the vortex period, the remaining blocking buffer in the corresponding reaction vessel was removed with a pipette and the contents of the tube (200 μL) were pipetted into the reaction vessel and placed into the magnetometer. In the matrix-effect experiments in the presence of pork meat, anti-TC Ab-PMPs were resuspended with an equal volume of pork solution and buffer spiked with TC resulting in a final concentration 1% *w/v* pork.

For each assay, as the concentration of anti-TC Ab-PMPs (and their impact on voltage readouts) was known, the number of surface-bound anti-TC Ab-PMPs could be used to reliably quantify TC concentration within a given sample. Based on previous papers [13–15,20], voltage shift values were calculated by subtracting 'Magnet Out' (O) values from initial 'Baseline' (B) values (Baseline-Magnet Out (B—O) (Fig. 4)) to determine the influence of PMPs on the magnetometer.

An initial incubation period before baseline readings allows the resonant coil sensor to stabilise (Fig. 4). At 60 s, the magnets are moved close to the sensor surface. PMPs within the reaction vessel are pulled down to the surface during the Magnet-In period (Fig. 4) where specific binding to pre-coated reaction vessel surfaces can occur, in turn impacting the resonant coil frequency of the magnetometer coil; this is illustrated by the monotonic decrease in output voltage. Once the magnet is retracted (Magnet-Out), unbound PMPs move away from the surface via Brownian motion and electrostatic repulsion, leaving only

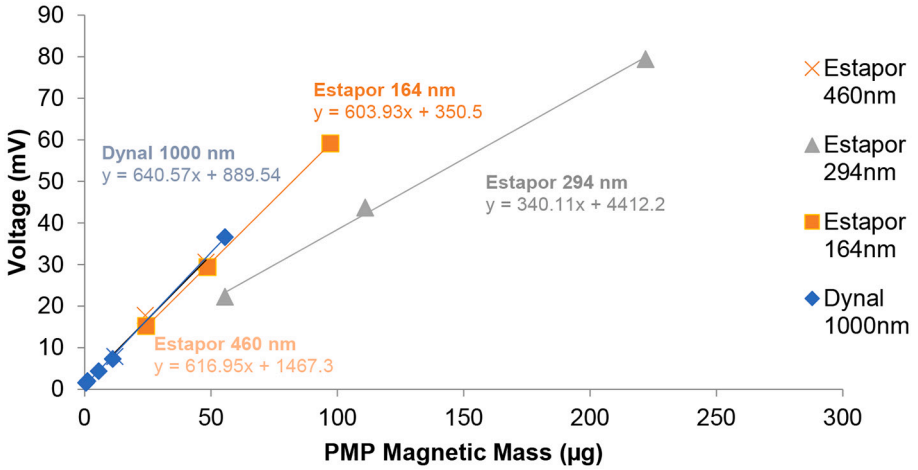

Fig. 3. Voltage shifts (Baseline-Out) in response to magnetic mass (μg) of paramagnetic particles from each supplier.

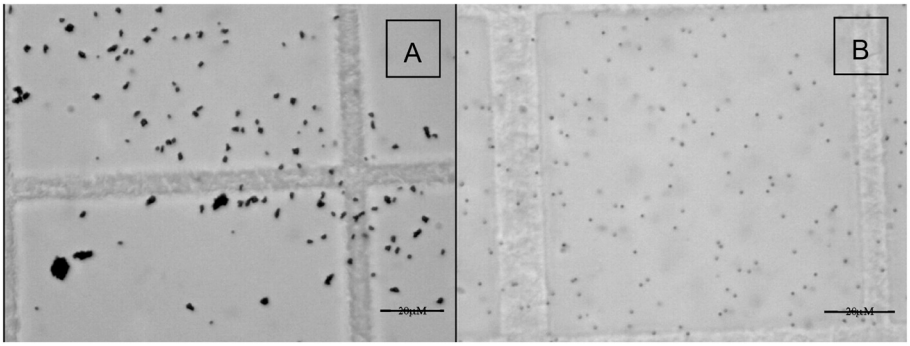

Fig. 4. Light microscope image of unsonicated (A; scale bar = 10 μM) and sonicated (B; scale bar = 20 μM) paramagnetic particles.

surface-bound PMPs; the change in recorded magnetic material on the surface results in a measurable shift in voltage (Fig. 4).

3. Results

Control and calibration experiments were performed with (1) an empty magnetometer, (2) an empty consumable, (3) a consumable with buffer and (4) a consumable with native PMPs to calibrate the device and inform MIA analysis. Changes in the number of surface-bound PMPs were used to accurately calculate sample analyte concentrations. Magnetometer calibration curves were generated for PMPs from each potential supplier before moving forward with functionalisation. Linear relationships ($R^2 = 0.999$ [Dynal; 1 μM], 0.999 [Estapor; 164 nm], 0.998 [Estapor; 294 nm] and 0.999 [Estapor; 460 nm]) between magnetic mass of PMPs and change in voltage (mV) were observed (Fig. 3). The magnet mass of PMPs was calculated by determining the mass/bead ratio and multiplying this by the known magnetite content. The sensitivity of response was based on the slope of the line of the response to magnetic mass. Dynal 1 μM, Estapor 460 nm and Estapor 164 nm all had similar responses but Dynal 1 μM (slope 640.57) had the best sensitivity, followed by Estapor 460 nm (slope 616.95) and then Estapor 164 nm (slope 603.93). Although similar, Dynabeads® MyOne™ tosyl-activated PMPs (Dynal; 1 μM) were selected as the PMPs to functionalise and use in the assay as they did not clump during the coating process, their rate of voltage change with increasing mass was superior and they had the greatest surface area (Fig. 3).

Optimised sonication protocols were critical in ensuring even PMP coating during antibody conjugation, consistent particle kinetics and analyte binding during assays. Fig. 4A shows PMPs without sonication. Fig. 4B shows the same PMPs after 4× (30s) sonication pulses with 60s intervals at 10 W on ice. Timed bursts and submersion in ice were essential to reduce overheating and maintain PMP and conjugated antibody functionality during sonication. Aggregated PMPs were shown to break apart and form mono-dispersed colonies after ultrasonic treatment. Aggregated PMPs exhibited unpredictable behaviour, with a clumping effect frequently observed in data trends. Clumped PMPs had a greater net impact on resonant coils, altered kinetics and reduced binding capacity across MIAs. Mono-dispersed PMPs were required to achieve optimum analyte-PMP binding ratios during assays and as such, PMPs were sonicated prior to assays to ensure homogenous solutions. To test stability, aliquots of PMPs at all stages of functionalisation were stored and evaluated over time; current data has confirmed PMP stability after six months (data not shown).

Different sensor surface treatments were trialed to evaluate modified sensor surface chemistry on antigen coating, PMP binding patterns and overall MIA outcomes. UV-treated and non-treated sensor surfaces were compared (Fig. 5). The non-treated surfaces gave the greatest response from the magnetometer, implying that higher amounts of BSA-TC was captured on the sensor surface. The fact that no competitive response is observed across the increasing TC concentrations can be ascribed to the high BSA-TC concentration on the surface. As later discussed, the ratio of BSA-TC and antibody loading on the particle surface must be carefully optimised for the concentration range of interest. For this work the non-treated sensor surfaces were opted for future assays which would also help the competitive costing of the final assay.

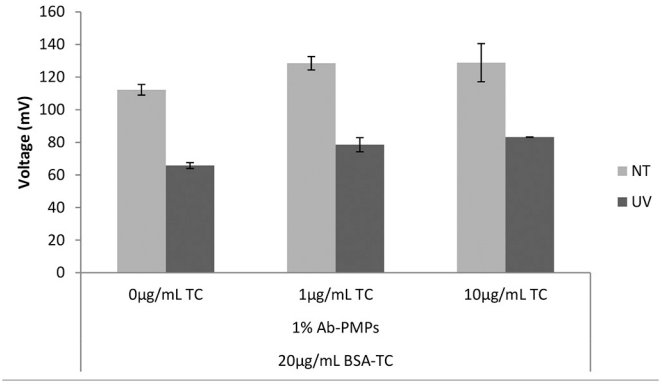

Fig. 5. Mean voltage shifts (+/− SE) (Baseline-Out) in response to 1% anti-tetracycline antibody coated paramagnetic particles on bovine serum albumin-tetracycline coated (NT - non-treated and UV - UV-treated) sensor surfaces with a tetracycline range, $n = 3$.

Different concentrations of BSA-TC were coated onto reaction vessel surfaces to determine the optimum coating concentration for MIAs; a fixed amount of anti-TC Ab-PMPs was used. Whilst percentage-change values were not significant between all tested BSA-TC concentrations ($P = 0.7538$; Kruskal-Wallis test), BSA-TC at 2.5 μg/mL, being the least concentrated and generating the lowest variability (Fig. 6), was chosen

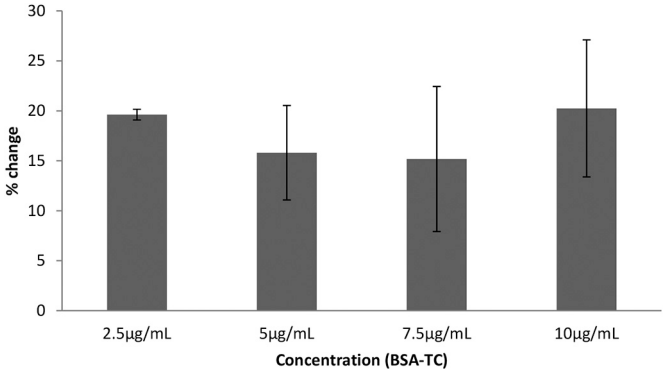

Fig. 6. Mean percentage-change (+/− SE) from 0 μg/mL bovine serum albumin-tetracycline (BSA-TC) controls after a magnetoimmunoassay of 1% anti-tetracycline antibody coated paramagnetic particles with a range of BSA-TC coated sensor surfaces, $n = 3$.

for all future assays. The increasing error associated with the measurement at higher BSA-TC loadings are thought to be due to excessive protein deposition on the surface causing the formation of unstable aggregates which are lost during the assay.

The formation of a PMP monolayer on the reaction vessel surface along with the correct antibody-to-analyte ratio was critical to assay functionality. At high (8.75×10^7/mL and above) and low (4×10^7/mL and below) concentrations, PMPs frequently generated no significant difference between control (0 μg/mL BSA-TC) and coated (2.5 μg/mL BSA-TC) sensor surfaces (data not shown); an outcome likely due to oversaturation of sensor surfaces and aggregation or, in the case of lower concentrations, small differences in the number of bound PMPs contributing little to overall mV shifts. High variability (again likely due to aggregation or non-specific binding) was regularly observed with antibody loading at high (1.5% and above) and low (0.5% (no lower coatings trialed)) coatings (data not shown). As such, PMPs at 1×10^7/reaction vessel [5×10^7/mL] with a surface coating of 1% mAb anti-TC were chosen as the optimal parameters for MIAs.

A dose response for TC-spiked assay and matrix-effect (1% meat suspension) buffer is shown in Fig. 7, where magnetometer response (baseline - magnet out; Fig. 1) is plotted against TC concentration of known standards over a 0-1 μg/mL range. Magnetometer cycles lasted a total of 8-min and no wash steps were required throughout the assay. Inhibition of 1% anti-TC Ab-PMP binding to 2.5 μg/mL BSA-TC coated reaction vessel surfaces by TC (0.1–1 μg/mL) was observed (Fig. 7). The data generated in Fig. 7 was used to determine an initial limit of detection for the spiked buffer and matrix-effect assay; work is on-going to further test the detection limits of the assay.

The high variation observed for anti-TC Ab-PMP incubated with TC at 1 μg/mL was likely due to the inherent noise of the magnetometer at lower voltages, in addition to the relatively fewer surface-bound PMPs. When the measurements were made in the presence of a 1% meat suspension, lower signals and greater variability were observed suggesting the influence of a matrix effect, with the possibility that anti-TC Ab-PMPs were impeded and/or TC was being absorbed by the 1% meat material present in the buffer.

In summary, at proof-of-principle stage our MIA is competitive in comparison with other methods of its class (Table 1), demonstrating analytical sensitivity and rapid readout times whilst requiring no wash steps or specially trained operators [13,20,23–25].

4. Discussion

The capability of a biosensor-based MIA method as an alternative to existing antibiotic screening systems was evaluated. TC, a frequently used drug in livestock populations, was the model antibiotic utilised for system development. In all livestock the acceptable limit of TC is between 100 μg/kg – 600 μg/kg depending on tissue origin [4,5,7]. The presence of TC above these thresholds can have implications for public health and increase the chances of antibiotic resistance both within humans and animal species [7,8]. Our system was capable of detecting TC-induced inhibition of anti-TC Ab-PMP binding to BSA-TC coated reaction vessel surfaces within the aforementioned range at a highly competitive readout time. Anti-TC Ab-PMP detection of TC-HRP within spiked buffer was successfully demonstrated in addition to detection within a 1% suspension of sonicated meat, highlighting resilience of assay components to matrix effects. Combined with previous work using PMPs as a dual role lysis-detection tool [20], these findings further support the use and transfer of this technique to detection of TC (along with other commonly used antibiotics) within livestock meat tissues and/or matrices.

Magnetometer detection limits were shown to fall in line with pre-set expectations [15,20], with voltage shifts in response to PMPs recorded as low as 6 mV (Fig. 7). Sonication drastically improved particle

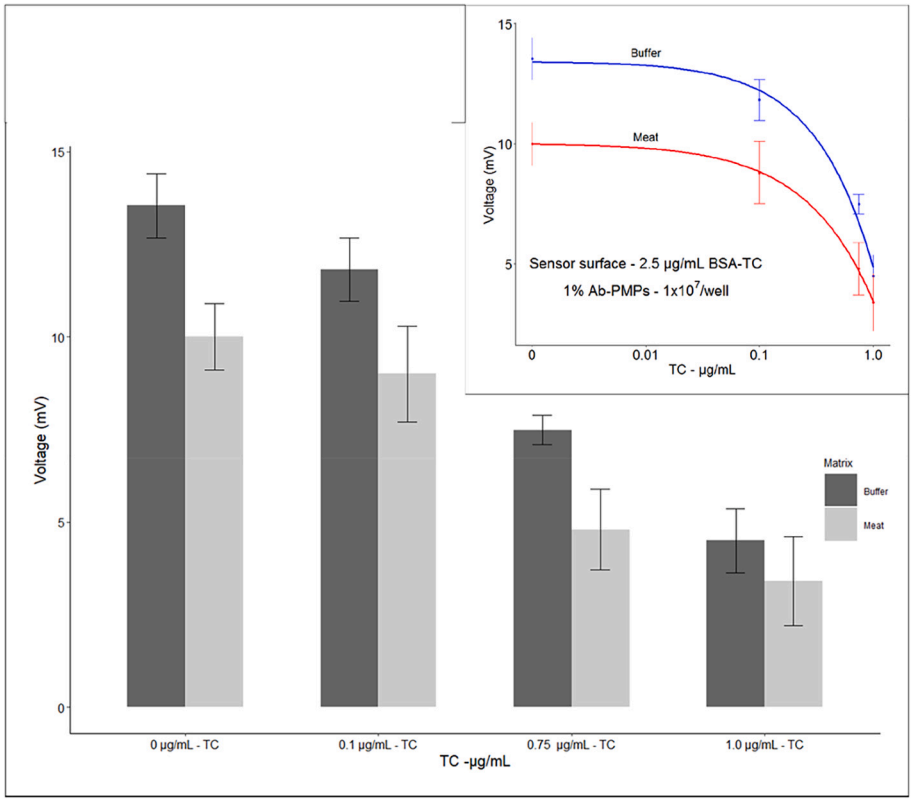

Fig. 7. Mean voltage shifts (+/− SE) (Baseline-Out) in response to 1% anti-tetracycline antibody coated paramagnetic particles on 2.5 μg/mL bovine serum albumin-tetracycline coated reaction vessel surfaces with a tetracycline concentration range in buffer and meat matrix, $n = 3$. The inset shows a 4-parameter logistic function curve fit for the data, used throughout the literature as an effective means against which to plot antibody-antigen interactions.

Table 1
Table comparing a high-pressure liquid chromatography (HPLC) 'gold-standard' methodology, different rapid detection techniques and our work, where LR = linear range and LOD = limit of detection. Greater than (>) used in instances where full details of sample treatment omitted.

Method/Application	Analytical Parameters	Readout	Advantages	Disadvantages	Ref.
HPLC with post-column derivatization and fluorescence detection of tetracycline in milk	LR: 0.005–5 μg/mL LOD: 5 ng/mL	>43 min	Analytically-sensitive	Expensive; time-consuming and labour-intensive sample treatment; expertise required	[23]
Biosensor-based generic dipstick technology for antibiotic detection in agricultural products	LR: 0.005 - 1 μg/mL LOD: 5 ng/mL	>35 min	De-skilled; analytically-sensitive; high-throughput; portable	High initial investment; limited accuracy; susceptible to biodegradation	[24]
Specific colorimetric aptasensor for rapid detection of tetracycline in raw milk using cysteamine-stabilized gold nanoparticles	LR: 0.2 μg/mL - 2 μg/mL LOD: 0.039 μg/mL	>36 min	Selective; portable	One-shot detection; susceptible to biodegradation; complex and time-consuming screening of small molecules	[25]
Visual and fluorometric lateral flow immunoassay combined with a dual-functional test mode for rapid determination of tetracycline antibiotics	LOD: 2 ng/mL [Buffer]; 40 μg/kg [Meat]	30 min (incl. Sample treatment)	Rapid; analytically-sensitive; dual readout	Laborious sample treatment; obstruction of pores from matrix components; visual readout susceptible to error	[26]
Biosensor-based detection of tetracycline in spiked buffer and meat using antibody-coated paramagnetic particles	LR: 0.1 μg/mL - 1 μg/mL. LOD (Visual): 0.1 μg/mL [Buffer and Meat]	20 min (incl. Sample treatment)	Rapid; high-throughput; low-cost; de-skilled; portable; analytically sensitive	Threshold-level sensitivity; early stage of development	Our work

performance and assay outcomes; a number of portable sonication devices exist which could later be incorporated as part of the assay [22]. Additionally, reaction vessel surfaces were successfully coated in BSA-TC at a range of concentrations, with consistent recognition of BSA-TC by anti-TC Ab-PMPs throughout MIAs; optimised reaction vessel surface chemistry was shown to be critical in reaching desired detection capabilities. Whilst the data strongly supports assay feasibility and gives scope for real-world applications, analytical parameters could be improved. Further optimisation of antibody conjugation methods and fine tuning of antibody percentage-coating on PMP surfaces alongside total PMP concentrations could further increase analytical-kit applicability, assay sensitivity and dynamic range. Refined BSA-TC surface coating could also help to improve MIA accuracy and reproducibility. Additionally, in order to vastly simplify the measurement process and in turn reduce readout times, future work aims to incorporate and sequentially perform ultrasonic extraction and measurement within the reaction vessel. Lastly, work to optimise meat processing and mixing with PMPs, combined with spike and recovery assays to evaluate the full extent of matrix effects could build on assay performance.

5. Conclusion

In conclusion, the project successfully demonstrated the feasibility of the proposed antibiotic detection technique whilst highlighting the need for additional work to be carried out in order to further optimise the system and explore other potential applications. Overall, the findings presented are promising and encouraging for the use of the magnetometer device and MIA technology as a rapid, novel and cost-effective antibiotic detection tool.

Author contributions

Mr. Owen Harrison carried out the investigation as part of an Innovate UK funded research project at the University West of England, in the Faculties of Health and Applied Science and Environment and Technology.

Mr. Bertrand Monnier's produced PMP magnetic mass calibration curves on the magnetometer device.

Prof Richard Luxton conceived the project, is a co-inventor of the magnetometer, and had oversight of assay development.

Prof Janice Kiely contributed to project design, is a co-inventor of the magnetometer and supervised the magnetometer development.

Dr. Dave West & Hugh Ballintine Dykes contributed to the project development and scope.

Dr. Ed Regan contributed to assay optimisation and assistance in the design of the assay cuvette.

Dr. Jeff Davey undertook the measurements in the presence of meat.

Funding

This research was funded by Innovate UK [Project. No. 242244].

Declaration of Competing Interest

The authors declare no conflict of interest.

Acknowledgments

The authors would like to thank Dr. Jacqueline Barnett and Galina Jönsson for proofreading this manuscript.

References

[1] V. Economou, P. Gousia, Agriculture and food animals as a source of antimicrobial-resistant bacteria, Infect. Drug Resist. 8 (2015) 49–61.
[2] I. Chopra, M. Roberts, Tetracycline antibiotics: mode of action, applications, molecular biology, and epidemiology of bacterial resistance, Microbiol. Mol. Biol. Rev. 65 (2) (2001) 232–260.
[3] K. Brown, R.R.E. Uwiera, M.L. Kalmokoff, S.P.J. Brooks, G.D. Inglis, Antimicrobial growth promoter use in livestock: a requirement to understand their modes of action to develop effective alternatives, Int. J. Antimicrob. Agents 49 (1) (Jan. 2017) 12–24.
[4] NOAH (National Office of Animal Health), Veterinary Medicines & the Safety of Food From Animals, Briefing Documents, 2016. Retrieved June 19, 2020, from, https://www.noah.co.uk/briefingdocument/veterinary-medicines-safety-food-animals/.
[5] The European Commission, Commission Regulation (EU) No 37/2010 of 22 December 2009 on Pharmacologically Active Substances and Their Classification Regarding Maximum Residue Limits in Foodstuffs of Animal Origin, 2010.
[6] S. Stead, et al., Meeting maximum residue limits: an improved screening technique for the rapid detection of antimicrobial residues in animal food products, Food Addit. Contam. 21 (3) (Mar. 2004) 216–221.
[7] N. Pastor-Navarro, Á. Maquieira, R. Puchades, Review on immunoanalytical determination of tetracycline and sulfonamide residues in edible products, Anal. Bioanal. Chem. 395 (4) (Oct. 2009) 907–920.
[8] World Health Organisation, Antimicrobial Resistance: Global Report on Surveillance, 2014.
[9] European Commission, The Rapid Alert System for Food and Feed 2017 Annual Report, 2017.
[10] S.G. Dmitrienko, E.V. Kochuk, V.V. Apyari, V.V. Tolmacheva, Y.A. Zolotov, Recent advances in sample preparation techniques and methods of sulfonamides detection – a review, Anal. Chim. Acta 850 (Nov. 2014) 6–25.
[11] C. Cháfer-Pericás, Á. Maquieira, R. Puchades, Fast screening methods to detect antibiotic residues in food samples, TrAC Trends Anal. Chem. 29 (9) (Oct. 2010) 1038–1049.

[12] S. Wang, H.Y. Zhang, L. Wang, Z.J. Duan, I. Kennedy, Analysis of sulphonamide residues in edible animal products: a review, Food Addit. Contam. 23 (4) (Apr. 2006) 362–384.
[13] E. Sharif, J. Kiely, R. Luxton, Novel immunoassay technique for rapid measurement of intracellular proteins using paramagnetic particles, J. Immunol. Methods 388 (1–2) (Feb. 2013) 78–85.
[14] J. Richardson, P. Hawkins, R. Luxton, The use of coated paramagnetic particles as a physical label in a magneto-immunoassay, Biosens. Bioelectron. 16 (9–12) (Dec. 2001) 989–993.
[15] J. Barnett, et al., An inexpensive, fast and sensitive quantitative lateral flow magneto-immunoassay for Total prostate specific antigen, Biosensors 4 (3) (Jul. 2014) 204–220.
[16] H. Hong, E.-G. Lim, J.-C. Jeong, J. Chang, S.-W. Shin, H.-J. Krause, Frequency mixing magnetic detection scanner for imaging magnetic particles in planar samples, J. Vis. Exp. no. 112 (2016).
[17] S. Li, L. Fu, J.M. Barbaree, Z.-Y. Cheng, Resonance behavior of magnetostrictive micro/milli-cantilever and its application as a biosensor, Sensors Actuators B Chem. 137 (2) (Apr. 2009) 692–699.
[18] W. Wang, Y. Wang, L. Tu, Y. Feng, T. Klein, J.-P. Wang, Magnetoresistive performance and comparison of supermagnetic nanoparticles on giant magnetoresistive sensor-based detection system, Sci. Rep. 4 (1) (May 2015) 5716.
[19] L. Ejsing, M.F. Hansen, A.K. Menon, H.A. Ferreira, D.L. Graham, P.P. Freitas, Magnetic microbead detection using the planar hall effect, J. Magn. Magn. Mater. 293 (1) (May 2005) 677–684.
[20] E. Sharif, J. Kiely, P. Wraith, R. Luxton, The dual role of paramagnetic particles for integrated lysis and measurement in a rapid immunoassay for intracellular proteins, IEEE Trans. Biomed. Eng. 60 (5) (May 2013) 1209–1216.
[21] C.A. Schneider, W.S. Rasband, K.W. Eliceiri, NIH image to ImageJ: 25 years of image analysis, Nat. Methods 9 (7) (Jul. 2012) 671–675.
[22] T.J. Tiong, L.E. Low, H.J. Teoh, J.-K. Chin, S. Manickam, Variation in performance at different positions of an ultrasonic VialTweeter – a study based on various physical and chemical activities, Ultrason. Sonochem. 27 (Nov. 2015) 165–170.
[23] I.D. Kargin, L.S. Sokolova, A.V. Pirogov, O.A. Shpigun, HPLC determination of tetracycline antibiotics in milk with post-column derivatization and fluorescence detection, Inorg. Mater. 52 (14) (2016) 1365–1369, https://doi.org/10.1134/S0020168516140065.
[24] N. Link, W. Weber, M. Fussenegger, A novel generic dipstick-based technology for rapid and precise detection of tetracycline, streptogramin and macrolide antibiotics in food samples, J. Biotechnol. 128 (3) (2007) 668–680, https://doi.org/10.1016/J.JBIOTEC.2006.11.011.
[25] Y. Luo, J. Xu, Y. Li, H. Gao, J. Guo, F. Shen, C. Sun, A novel colorimetric aptasensor using cysteamine-stabilized gold nanoparticles as probe for rapid and specific detection of tetracycline in raw milk, Food Control 54 (2015) 7–15, https://doi.org/10.1016/J.FOODCONT.2015.01.005.
[26] W. Sheng, Q. Chang, Y. Shi, W. Duan, Y. Zhang, S. Wang, Visual and fluorometric lateral flow immunoassay combined with a dual-functional test mode for rapid determination of tetracycline antibiotics, Microchim. Acta 185 (9) (2018) 404, https://doi.org/10.1007/s00604-018-2945-9.